2022 IEEE/RSJ International Conference on Intelligent Robots and Systems (IROS)
October 23-27, 2022, Kyoto, Japan

Design of a Reconfigurable Robot with Size-Adaptive Path Planner

S. M. Bhagya P. Samarakoon, M. A. Viraj J. Muthugala, Manivannan Kalimuthu,
Sathis Kumar Chandrasekaran and Mohan Rajesh Elara

Abstract— **Area coverage is demanded from the robots utilized in application domains such as floor cleaning. Even though many advanced coverage algorithms have been developed, the area coverage performance is limited due to the inaccessibility of narrow spaces caused by physical constraints. Reconfigurable robots have been introduced to overcome this limitation where reconfigurability could help in assessing narrow spaces. Nevertheless, the state-of-the-art reconfigurable robots are not capable of changing the morphology size and shape as a single entity. Therefore, this paper proposes a novel design of a reconfigurable robot with a size-adaptive coverage strategy. The reconfiguration mechanism is designed in such a way that the robot can independently expand or shrink its size along the principal planar axes, where the behavior allows the change of size and shape. The coverage strategy is based on boustrophedon motion and the A* algorithm modified for accessing narrow areas using the size adaptability. The design of the robot is detailed in the paper, including electro-mechanical aspects, design considerations, and the coverage path planning method. Experiments have been conducted using a prototype of the proposed design to analyze and evaluate the characteristics and the performance of the robot. The results show that the proposed robot design can improve the productivity of a floor cleaning robot in terms of area coverage and coverage time.**

Index Terms— **Area coverage, Path planning, Reconfigurable robotics, Robot design**

I. Introduction

Area coverage is essential for applications such as painting [1], cleaning [2], land mine detection [3], disinfection [4], and agriculture [5]. The robots intended for coverage applications are expected to maximize the productivity in terms of coverage time and energy usage in addition to area coverage performance [6]–[8]. According to the survey [9], many coverage path planning algorithms have been developed for robots. Boustrophedon motion, grid-based local, and contour line-based coverage path planning methods provide heuristic solutions for known environments and are computationally light weight [10]. On the other hand, neural network-based coverage methods have shown versatility in online coverage path planning in partially known environments even though the methods are computationally expensive [11]. Guruprasad and Ranjitha [12] proposed an approximate cellular decomposition-based online complete coverage planning algorithm for a mobile robot. According to [13], coverage path planning with minimal robot turns for covering all the points in the workspace could lead to higher productivity.

Avoiding complete battery draining and automatic charging are vital for robots used in coverage applications since the robots are continuously operated for a prolonged time. In this regard, the work [14] proposed an online coverage planning method for a mobile robot considering its battery status. The method is capable of navigating a robot toward a charging status before the battery is fully drained during a coverage application. Work on multi-robot optimum coordination to cover a given area could also be found in literature [15]. The difficulties of having a multi-robot system for coverage are the high cost of deployment and complex control. Even though much work has been done on algorithmic development to improve the coverage performance, as discussed above, the area coverage is limited by the inaccessibility of narrow spaces due to physical constraints.

The work [16] reviewed the development of reconfigurable robots and synthesized potential applications as well as challenges. According to the implication of the review, reconfigurable robots have a great potential for area coverage applications. Furthermore, a new class of hinged reconfigurable robots, that are intended for floor cleaning applications can be found in the literature [7], [17], [18]. Path planning, coverage, energy usage and reconfiguration strategies of these tiling robots have been explored in the cited work. Furthermore, the work [19] proposed a conceptualized hinged reconfigurable robot that can change its size. However, hardware design for realizing the concept has not been proposed. In addition, the size is considered fixed for covering a region during the simulation-based validation. The main limitations of the hinged reconfigurable robots are the complexity of control and autonomy, less durability, and higher deployment cost caused by the serially connected complex electro-mechanical systems. For example, the hinged reconfigurable robot presented in [17] has four omnidrive blocks connected serially, which is almost equivalent to four individual modular robots.

Various types of shapes and size transformations can be observed in the domains of modular robotics [16]. The transformations are executed by connecting and disconnecting the modules [20]. These modular robots are less feasible for coverage applications. For example, deployment cost of the system would be high since each module should have locomotion modules, perception, processing, and communication abilities. A robot with variable polygon size based on a variable topology truss has been introduced in [21].

This research is supported by A*STAR under its Industry Alignment Fund – Pre Positioning (Award M21K1a0104), and National Robotics Programme under its Robot Domain Specific (Funding Agency Project No. W1922d0110) and administered by the Agency for Science, Technology and Research.

The authors are with the Engineering Product Development Pillar, Singapore University of Technology and Design, Singapore bhagya_samarakoon@mymail.sutd.edu.sg

2022 IEEE/RSJ International Conference on Intelligent Robots and Systems (IROS) | 978-1-6654-7927-1/22/$31.00 ©2022 IEEE | DOI: 10.1109/IROS47612.2022.9981125

Here, truss members are connected by linearly actuated truss members and passive rotational joints. The robot can change its size to adapt to the environment. Although the robot is aligned with inspection purposes it is ineffective for coverage applications such as floor cleaning and disinfection since it is merely a truss with links and joints.

Robots intended for indoor area coverage problems should be able to cope with unstructured environments. Accessing both larger spaces and narrow spaces are expected from the robots during their coverage tasks. A single module robot that could fit into these requirements could lead to higher productivity in coverage. However, such a robot and a path planner have not been designed and developed yet. This paper proposes a novel design of a reconfigurable robot with size-adaptive path planning. The size-adaptive coverage strategy allows the robot to access narrow spaces by shrinking and covering uncluttered areas with an expanded form. The design considerations of the robot are explained in Section II. Particulars on the electro-mechanical systems of the proposed robots are detailed in Section III. The coverage strategy proposed for the robot is explained in Section IV. Experimental validation is discussed in Section V. Finally, concluding remarks are presented in Section VI.

II. Robot Design Considerations

Area coverage and coverage time are crucial performance indicators for a robot intended for coverage applications [6]–[8]. Often, they are conflicting factors. Furthermore, area coverage and coverage time are heavily dependent on the effective size of a robot. This phenomenon could be further explained with the aid of the situation depicted in Fig. 1(a) where a robot with a higher size covers an environment. Since the robot size is high, it requires a lesser number of steps to cover the environment. However, a considerable amount of area is left uncovered since the robot could not access the narrow spaces resulted from obstacles such as furniture. In contrast, a robot with a lower size can have a higher area coverage compared to the large robot since it could access the narrow spaces that could not be assessed by the larger robot. Nevertheless, coverage time would be considerably higher compared to the larger robot since the robot requires a higher number of steps to cover the area. Thus, the coverage time and area coverage can be a tradeoff with the size of the robot used in a coverage application.

A robot that can reconfigure its size would be a perfect solution for maximizing the performance in terms of area coverage and coverage time since the adaptability of the size can efficiently trade off these two conflicting entities. For example, a situation of a robot that can reconfigure its size covers the example environment is considered (see Fig. 1(c)). The robot covers the free areas of the environment while maintaining its large morphology to reduce the steps required for coverage. In the encounters of narrow spaces created by obstacle clusters, the robot reconfigures into a smaller morphology that allows it to access the narrow spaces. Therefore, the ability to change the morphology size is considered the main design ideology of the proposed

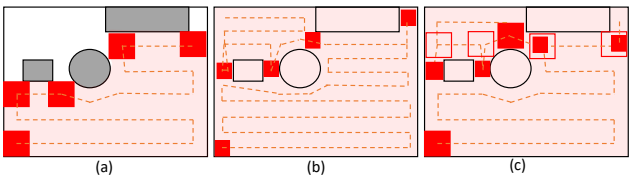

Fig. 1. Explanation of trade off between area coverage and coverage size based on morphology size. (a) A robot large in size cover an environment, (b) A small robot covering the environment, and (c) A robot that can reconfigure its morphology size cover the environment. Shaded red color represent the coverage. The red square represent the robot. The scenarios of size changing from maximum size to smaller sizes are indicted by non-filled squares. The robot's navigation path indicated by dashed-line are illustrations for the sake of explanations.

robot. Apart from that, the following design aspects were considered for the robot.

- The ability change the size in a continuous way rather than a few step of sizes would be favourable for the efficiency of the coverage since the dimensions of narrow spaces have a greater variability.
- The ability of the robot to change the morphology shape would complement flexibility and improve the efficiency of coverage.
- The ability to maintain the shape and the size without continuously activating the actuators is useful on improving the energy efficiency.
- The robot's size range should be comparable to the indoor environments where the robot is expected to be deployed for area coverage. The minimum to maximum footprint size ratio should be high enough (above two times) to have a considerable impact.
- Making the robot as a single module reduces the cost and the complexity of the deployment compared to a multi-robot modular system that requires multiple sensing units, locomotion units, and intercommunication. Furthermore, all the sensors, actuators, and processing modules should be compacted within the robot.

III. Robot Platform Design

A. Mechanical Design

The robot design is divided into three different sub-assemblies, 1) Traction unit, 2) Reconfiguration unit, and 3) Robot enclosure. The exploded isometric view of the robot is shown in Fig. 2(a). The traction unit consists of three brushed DC geared motors (11 V, 82.3 rpm, 5.1 kgcm) with incremental encoders coupled with omni wheel with diameter of 50 mm, to drive the robot. Each motor and wheel is placed 120° apart to enable the omnidirectional drive. Besides, the locomotion unit is designed to carry a payload of 3 kg with a safety factor of 1.5.

The reconfiguration unit enables the robot to vary its morphology. During the fully shrunk stage, the length, width, and height of the robot are 20 cm × 20 cm × 22.5 cm. While in the fully expanded stage, the length, width, and height of the robot are 30 cm × 30 cm × 22.5 cm respectively. The fully shrunk and expanded state of the robot are depicted in Fig. 2(b). It should be noted that the reconfiguration is

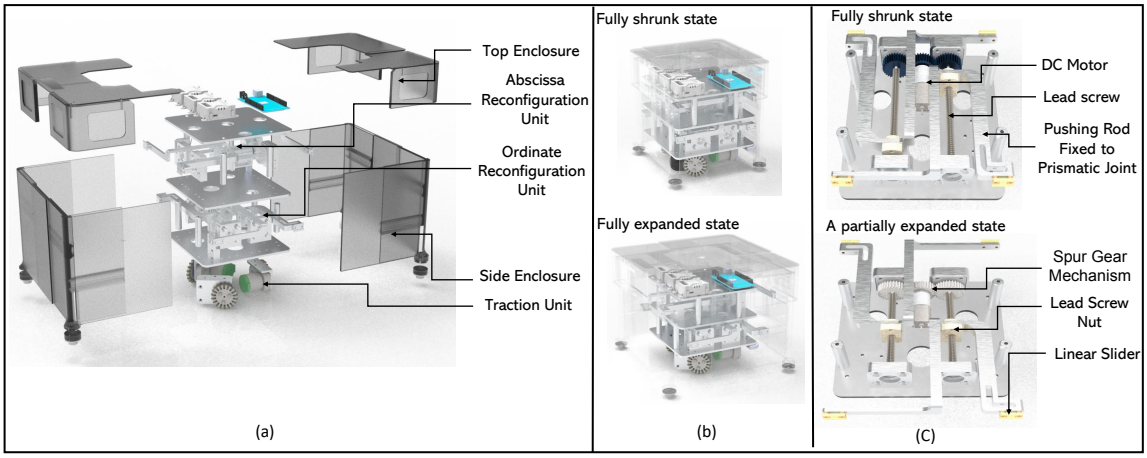

Fig. 2. (a) Exploded isometric view of the robot. (b) 3D CAD model of the robot in fully shrunk and expand states. (c) A reconfiguration unit.

not limited to two states and the mechanism allows the robot to reconfigure into any size within the minimum and the maximum range. A pair of independent actuation units with a lead screw mechanism is used to vary the robot's length in X and Y directions, as shown in Fig. 2(c). The self-locking ability of the lead screws allows the robot to maintain the morphology without continuously energizing the actuators. This behavior is useful for saving energy as well as simplifying the control. In a reconfiguration mechanism, the transmission from the brushed DC geared motor (12 V, 110 rpm, 7.8 kgcm) is split into two outputs using a spur gear mechanism. Two spur gears turn the lead screw with a pitch of 10 mm. The pushing rod at one end is connected to a lead screw nut and the other with a prismatic joint, which is connected to the outer cover, that allows the robot to expand/shrink simultaneously in two directions. The expansion mechanism uses a helix threaded lead screw to enable the robot to expand/shrink faster.

Robot skin is divided into four independent segments, each connected to the reconfiguration mechanism by a linear slider. At the end of the four segments, ball caster units are attached for support and restricts the sagging of the outer cover. To keep the robot light weighted, the outer skin of the robot is 3D printed using Polylactic Acid (PLA) material by exploiting the Fused Deposition Modelling (FDM) technique. The top enclosure is designed to install a LIDAR. Apart from that, the robot is designed with the provision to install task-oriented payloads such as cleaning mechanisms.

B. System Architecture

The electrical/electronics system of the robot is depicted in Fig. 3. A microcontroller (Arduino Mega 2560) is used as the central processing unit of the robot at the current state. The microcontroller communicates with motor drivers (Roboclaw 2×7A) through Transistor-Transistor Logic (TTL) serial communication to actuates the DC motors used for reconfiguration (denoted as R1 and R2), and locomotion (denoted as L1, L2, and L3). The DC motors used for reconfiguration and locomotion consist of quadrature encoders (12 counts per revolution before gear ratio). These encoders are connected

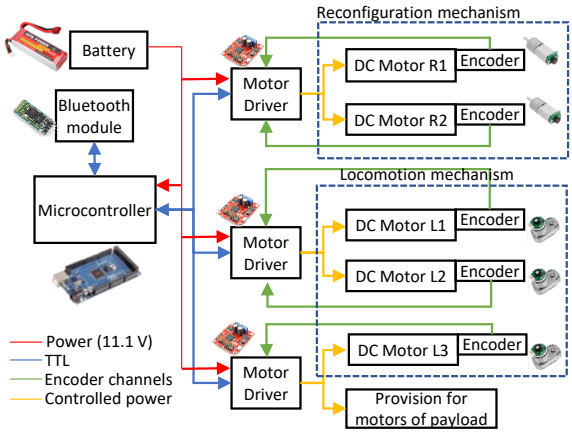

Fig. 3. Electrical/electronic system

to the corresponding motor driver, and the motor drivers internally perform the quadrature decoding to measure the movements. In the case of reconfiguration, the rotational movements are calibrated to the translations of the lead screw mechanisms to measure the length of the robot along the X and Y axes (L_X and L_Y, respectively). A Bluetooth module (HC-05) connected to the microcontroller through TTL serial is used to communicates wirelessly with a remote terminal. All the components are powered by an 11.1 V 2200 mAh Li-Po battery that is sufficient for about two hours of a continuous run of the robot after a charge. The system has provisions to install a compute stick for high-level decision-making and a LIDAR for perceiving the environment.

The control block diagram of the robot is depicted in Fig. 4. For a given reconfiguration size ($(L_X)_{t_f}$ and $(L_Y)_{t_f}$), the trajectory generator produces a smooth reference time-position profile (i.e., L_X^* and L_Y^*). The cubic polynomial approach [22] is used for trajectory planning where t_f is the specified time duration. Then, each motor attached to the reconfiguration is controlled by a Proportional Integral Derivative (PID) controller to follow the reference position command. In the case of locomotion, the velocity commands given with respect to the robot (i.e., V_X, V_Y, and ω) are

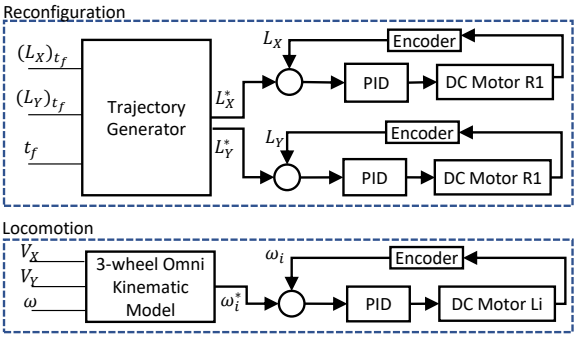

Fig. 4. Control block diagram

converted to reference angular velocity of each drive motor (ω_i^* for $i = 1, 2, 3$) using the 3-wheel omni kinematic model [23]. Each drive motor is controlled through a closed-loop PID controller to actuates it per the reference angular velocity command. Reconfiguration and velocity commands are expected to be received from an autonomy layer or user interface.

IV. Size-Adaptive Coverage Strategy

The size-adaptive coverage strategy for the proposed robot has been developed considering a combination of boustrophedon motion and the A* algorithm. The existing coverage methods built upon the boustrophedon motion and the A* algorithm (e.g., [24]) are not capable of adapting the size of a robot. Therefore, the standard boustrophedon and the A* algorithm have been modified to allow size adaptability. The proposed coverage strategy considers that the robot's width and length are equivalent. Thus, the robot size is defined as L_R such that (i.e., $L_R = L_X = L_Y$). For the sake of simplicity of formulation and computation, it is assumed that the robot's size (i.e., L_R) can be changed to only two states, the fully expanded (L_R = largest) and the fully shrunk (L_R = smallest). The flow of the proposed coverage strategy can be explained with the aid of Fig. 5 and Algorithm 1.

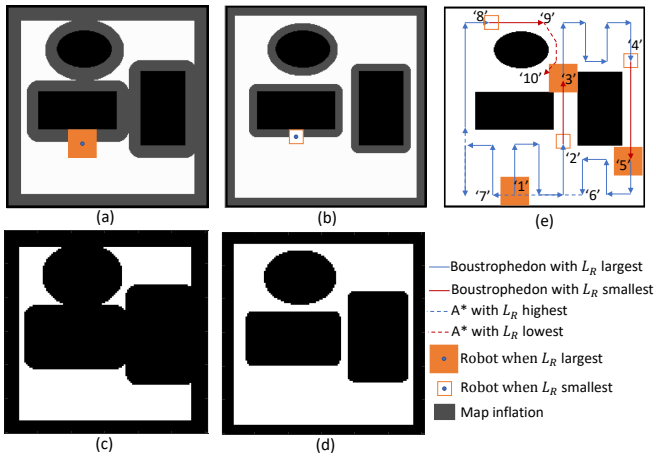

Fig. 5. Size-adaptive coverage strategy. (a): Inflated metric map per the largest size of the robot, (b): Inflated metric map per to L_R highest, (c) Occupancy grid map corresponding to (b), (d): Occupancy grid map corresponding to (c), and (e) An example path of the robot.

Algorithm 1: Size-Adaptive Coverage Strategy

input : metric map
output: coverage path, robot size
Generate inflated maps for L_R = Largest, Smallest;
Generate obstacle inflated map for L_R = Smallest;
Generate occupancy grid maps, G^L and G^S;
(X_R, Y_R) = Initial position;
while *(There are uncovered cells)* **do**
  dead end met = False;
  while *(! dead end met)* **do**
    if $(X_R, Y_R + 1)$ *in* G^L *is uncovered* **then**
      L_R = Largest;
      $Y_R = Y_R + 1$;
    else if $(X_R, Y_R + 1)$ *in* G^S *is uncovered* **then**
      L_R = Smallest;
      $Y_R = Y_R + 1$;
    else if $(X_R, Y_R - 1)$ *in* G^L *is uncovered* **then**
      L_R = Largest;
      $Y_R = Y_R - 1$;
    else if $(X_R, Y_R - 1)$ *in* G^S *is uncovered* **then**
      L_R = Smallest;
      $Y_R = Y_R - 1$;
    else if $(X_R + 1, Y_R)$ *in* G^L *is uncovered* **then**
      L_R = Largest;
      $X_R = X_R + 1$;
    else if $(X_R + 1, Y_R)$ *in* G^S *is uncovered* **then**
      L_R = Smallest;
      $X_R = X_R + 1$;
    else if $(X_R - 1, Y_R)$ *in* G^L *is uncovered* **then**
      L_R = Largest;
      $X_R = X_R - 1$;
    else if $(X_R - 1, Y_R)$ *in* G^S *is uncovered* **then**
      L_R = Smallest;
      $X_R = X_R - 1$;
    else
      dead end met = True;
    end
  end
  Find paths to uncovered cells in G^L using A*;
  if *(A path exists in* G^L*)* **then**
    L_R = Largest;
    Select the shortest path;
    (X_R, Y_R) = sequence of A* algorithm;
  else
    Find paths to uncovered cells in G^S using A*;
    if *(A path exists in* G^L*)* **then**
      L_R = Smallest;
      Select the shortest path;
      (X_R, Y_R) = sequence of A* algorithm;
    else
      End coverage;
    end
  end
end

The algorithm takes the metric map of the environment as an input. This map can be created from LIDAR information. Two distinct maps are generated by inflating the obstacle in the metric map considering the two size states of the robot. The amount of inflation is taken as $L_R/2–a/2$, where a is the cell size such that $a < L_R$. The inflated maps corresponding to the robot's largest and smallest sizes are given in Fig. 5(a) and (b), respectively. This amount of inflation ascertains the collision-free navigation and coverage near the obstacle boundaries (see the robot near the obstacle in Fig. 5(a) and (b)). Then, two occupancy grids maps corresponding to the inflated maps are generated considering a uniform grid as shown in Fig. 5 (c) and (d). The same cell size is considered here for the cases of L_R = largest and L_R = smallest. G^L and G^S denote the two occupancy grid maps for the event of largest and smallest, respectively.

The robot starts the boustrophedon motion from its initial position, where the robot's current position is denoted by (X_R, Y_R) (see '1' in Fig. 5(e)). The next location for the movement is first checked on the direction of Y-axis based on G^L. If the cell $(X_R, Y_R + 1)$ is uncovered, the robot moves to that cell. Otherwise, the robot check $(X_R, Y_R + 1)$ of G^S. When the movement is based on G^S, the robot size (L_R) is reconfigured to the smallest size (e.g., '2', '4', and '8' in Fig. 5(e)). Otherwise, the robot is configured to the largest size (see '1','3', and '5' in Fig, 5(e)). Similarly, the robot checks the possible movement in all the four principal axes. If a dead-end is met (i.e., no neighboring uncovered cell in the four-principle directions of (X_R, Y_R) in both G^L and G^S), the boustrophedon motion is ended (see '6' in Fig. 5(e)). Then, the robot searches collision-free navigation paths for remaining uncovered cells in G^L using the A* algorithm. If a path exists, the robot moves to a new cell using the shortest path found by the A* algorithm considering its largest configuration (e.g., '6' to '7' in Fig. 5(e)). If no path is found in G^L, the robot explores paths in G^S using the A* algorithm. In the event of G^S, the robot moves along the path returned by the A* algorithm considering the smallest size (e.g., '9' to '10' in Fig. 5(e)). After navigating to a new cell, the boustrophedon motion is restarted. This process is repeated until all the cells are covered, or no A* path exits in both G^L and G^S.

Neighbourhood cells are also covered when the robot is in a particular cell since $a < L_R$. Therefore, the neighboring cells that the robot would physically cover are tagged as covered during the robot movement if a neighborhood cell is not adjacent to an obstacle cell. The covering neighborhood is varied with the robot's size configuration at each step. Even though this algorithm has been formulated considering only two size configurations, it can be extended for intermediate size configuration by considering additional occupancy grid maps. For example, if n size configurations were chosen, n occupancy grid maps should be generated considering the inflated maps corresponding to the selected size configurations.

V. Results and Discussion

A. Reconfiguration characteristics

The first set of experiments has been conducted to assess the compliance of the reconfiguration characteristics with the design considerations. The robot was initially placed on the ground in its smallest size (both X-axis and Y-axis shrink to a minimum, and the execution of the robot reconfiguration was recorded as shown in Fig. 6. Furthermore, the length of the robot along X and Y axes (denoted as L_X and L_Y, respectively) were measured through the encoder readings of the corresponding reconfiguration motors are also plotted in Fig. 6 along with reference trajectories.

In case 'a', the robot was operated to expand only along the Y-axis of the robot. A sequence of snapshots taken during this run and the corresponding trajectories of the robot length along the X and Y axes are given in Fig. 6(a). The reconfiguration of the robot along the X-axis is considered for case 'b'. The snapshots and trajectories corresponding to this case are given in Fig. 6(b). The expansion and shrink reconfiguration along one axis could be used to change the shape of the robot as well as the size. The obtained results confirm that the robot is capable of reconfiguring per the command where the robot follows the reference trajectories without any issues. In case 'c', synchronous reconfiguration along both X and Y axes was considered. According to the obtained results (shown in Fig. 6(c)), the robot is capable of reconfiguring its size while maintaining the morphology aspect ratio (width to length ratio) in a given value.

Similar to these three cases, the shrinking and expansion of the robot from any arbitrary configuration, reconfiguring to any intermediate positions, and shrinking one axis while expanding the other axis were also performed. The characteristics and the operation of the robot in these scenarios are almost the same as the cases discussed here. Hence, the results are not explicitly presented in the paper. In all the cases, the robot was capable of reconfiguring without any issues. Following salient characteristics could be identified from the analysis of the experimental observations.

- The shrink and expansion can range from 20 cm to 30 cm, which leads to the maximum size to minimum size ratio in terms of footprint area is more than two times. Thus, size adaptability can impact area coverage and coverage time performance considerably.
- The reconfiguration is continuous, and the robot can reconfigure its dimension to any value within the minimum and maximum range initiating from any size configuration.
- The time taken for reconfiguring from the fully shrunk to the fully expanded was on average 6.74 s (standard deviation = 0.05). This observation implies that the reconfiguration speed is adequate for the intended application, where the time for reconfiguration is negligible compared to typical coverage time on environments.
- The expansion of one axis while shrinking the other axis could also be performed.

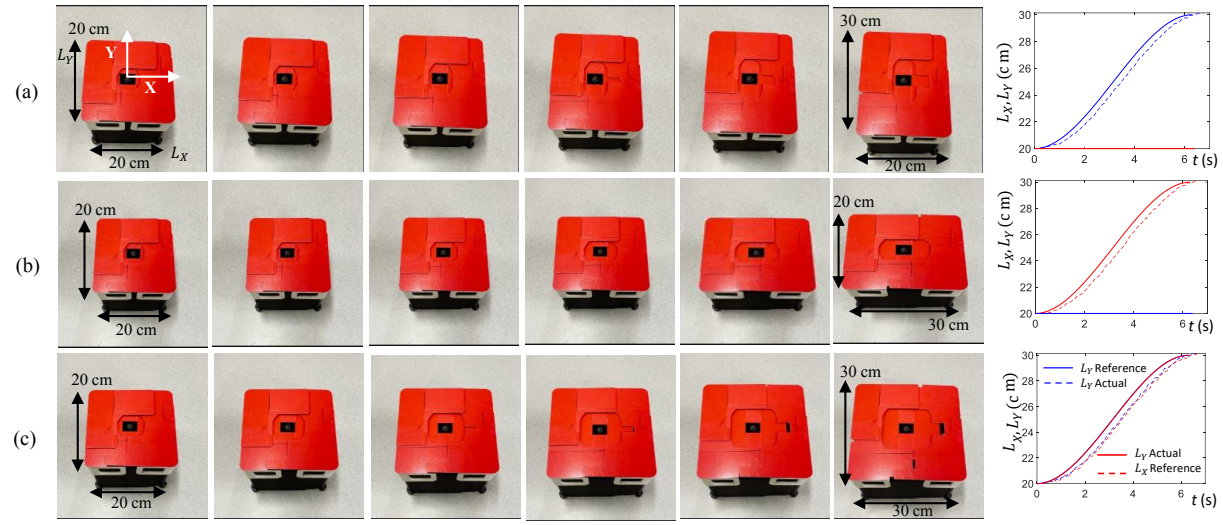

Fig. 6. The image sequence of the size reconfigurations and the corresponding trajectories. (a) Robot size reconfiguration sequence Y-axis. (b) Robot size reconfiguration sequence in X-axis. (c) Robot size expands in X and Y axes.

- The reconfiguration is smooth, and no mechanical hindrances for the movements were noted.

Therefore, it can be concluded that the observations of the first set of experiments validate that the ability of the proposed mechanism in changing the morphology size and shape. Furthermore, the characteristics of the reconfiguration comply with the design considerations (see Section II) intended for the robot.

B. Performance Evaluation

The second set of experiments was conducted to evaluate the performance gain of the proposed robot over robots with fixed sizes. This set of experiments was conducted in a laboratory setting that replicates a typical arrangement of a discussion layout with scattered furniture. The size of the experimental environment was 3.2 m $\times$ 2.4 m. The layout of the test environment is shown in Fig.7. Three runs of the robot with distinct configurations for area coverage were considered. In the first run, the robot was operated considering its ability to reconfigure its morphology size. The second and third runs were performed to benchmark the performance gain of the reconfiguration ability compared to robots with fixed morphology size. The configurations of the robot fixed to its maximum (30 cm $\times$ 30 cm) and minimum size (20 cm $\times$ 20 cm) were considered for these baseline cases where the reconfiguration ability was disabled. The robot was run with the same linear velocity during the three runs to maintain the homogeneity across the runs other than morphology size. Area coverage and coverage time of these three runs were compared to access the performance gain of the proposed morphology size reconfiguration.

Initially, a simulation study was conducted considering the metric map of the environment. The simulated robot paths and configurations as well as coverage results during the three runs are depicted in Fig. 8. The run of the robot with the ability of size adapting achieved area coverage of 97% while the robot fixed to the smallest size achieved 97%. In contrast, the robot fixed to the largest size could achieve only 63%. Even though the coverage performance of the robot fixed to the smallest size and the robot with size-adaptive ability reported almost the same coverage, the run of the robot fixed to the smallest size demanded considerably higher coverage time (24.4 min for the event of fixed to the smallest size and 15.27 min for the run of size adaptability). These coverage times were obtained by considering time taken by the robot for reconfigurations and navigation.

After the simulations, real robot deployment was considered. An overhead camera (1080P with 60 fps) was placed to analyze coverage within the environment. The robot was operated per the path and size configurations found out in the simulations. The key locations within the environment where the reconfiguration ability played a vital role during the area coverage are annotated by red color circles in Fig. 7. The robot's actions and consequences at the first three key locations, 'A', 'B', and 'C', are given in Fig. 9 for explaining the performance gain on area coverage due to the reconfiguration ability. For example, in location 'A', the robot encounters a narrow space caused by a chair leg and a

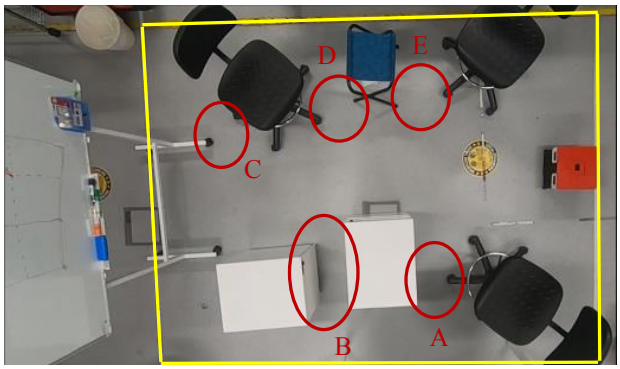

Fig. 7. The experiment environment is depicted here. The red-colored circles represent the narrow spaces that occurred in the environment.Yellow colored square represent the workspace considered for the area coverage.

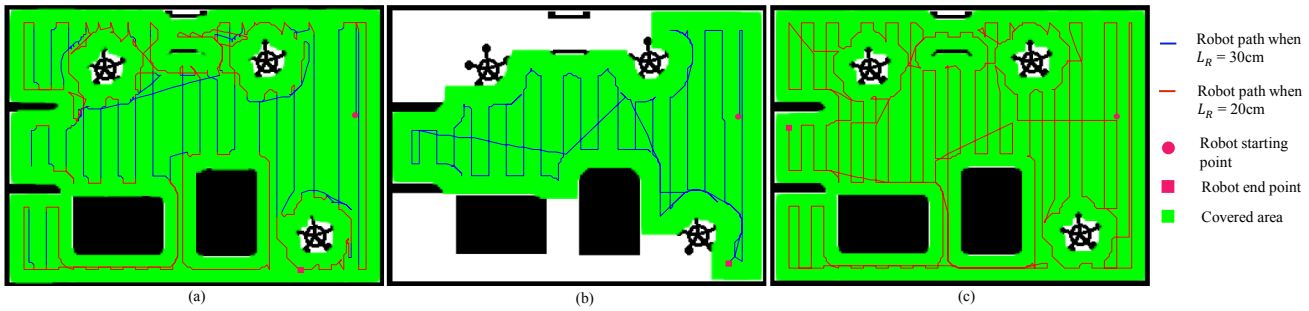

Fig. 8. Simulation results. (a): Robot with size reconfiguration ability, (b): Robot fixed to the smallest size, and (d): Robot fixed to largest size.

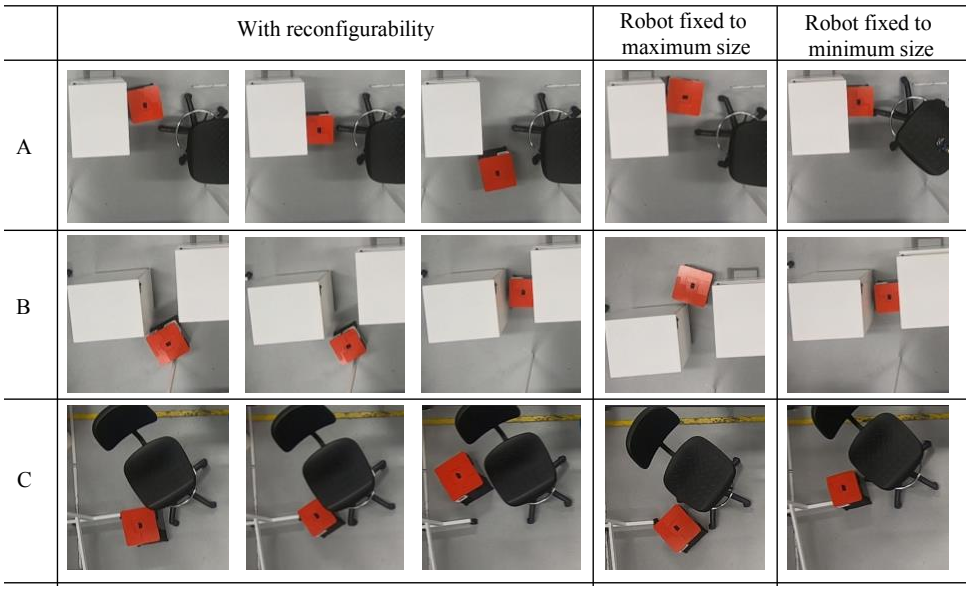

Fig. 9. The comparison between robot actions and consequences of the three runs at sample key locations.

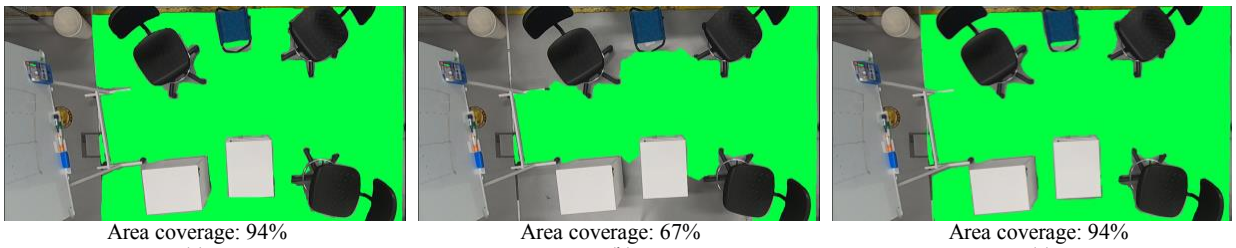

Fig. 10. Area coverage comparison of the three configurations of the robot during the robot deployment. (a) Robot with size reconfigurable ability, (b) Robot fixed to its maximum size, and (c): Robot fixed to its minimum size.

drawer. Here, the robot could not move through the narrow space when it is in its maximum size. In the case of the robot with adaptability, the size of the robot is reconfigured to the smaller size allowing the movement through it (see Fig. 9) for coverage. Thus, the reconfiguration allows the robot to access the narrow area for coverage. However, the robot could not access the area when it was fixed to the maximum size, yielding a considerable amount of uncovered area. In the run of the robot fixed to the smallest size, the robot could easily access the area. Nevertheless, the robot had to move more times in other areas since the robot size was smaller. A similar behavior could be observed throughout the experiment (see Fig. 9 for other sample scenarios).

The area coverage traced by analyzing the overhead camera feed of the three runs of the robot are depicted in Fig. 10 along with the percentage area coverage. The least area coverage performance was observed from the run of the robot fixed to the maximum size, where the area coverage was 67%. This poor area coverage resulted due to the inaccessibility of the narrow spaces due to size constraints. On the other hand, in the run of the robot with reconfiguration ability (i.e., the robot can shrink and expand) could achieve a percentage area coverage of 94%. This area coverage performance was equivalent to the robot

fixed to its minimum size. The robot achieved this amount of higher area coverage due to its ability to access narrow spaces. Nevertheless, the coverage time of the robot with reconfiguration was observed as 18.71 minutes which is remarkably lower than that of the run of the robot fixed to its minimum size (coverage time of the robot fixed to its minimum size was 29.34 minutes). This sort of higher performance from the coverage time could be achieved from the robot with reconfiguration ability since the robot managed to cover the noncongested areas through its maximum size and narrow areas with the small size. Moreover, morphology size reconfiguration allows the robot to maximize the area coverage performance while improving the performance in terms of coverage time. Therefore, the proposed novel robot design that can reconfigure its morphology size and shape improves the performance of area coverage applications such as floor cleaning in terms of area coverage and coverage time.

VI. Conclusions

A novel design of a reconfigurable robot and a size-adaptive coverage strategy have been proposed. The ability to adapt size as a single module during the coverage path planning is the major improvement of the proposed design over the state-of-the-art.

The proposed hardware design allows the robot to expand or shrink along the two planar principal axes that can be controlled independently. This independent reconfiguration ability is useful for changing the morphology shape in addition to the change of morphology size. Furthermore, the robot does not require continuously energizing the actuators responsible for the reconfiguration after a reconfiguration. This design consideration could be helpful for the durability of the reconfiguration mechanism and in saving energy.

The coverage path planning algorithm has been developed, combining the boustrophedon motion with the A* algorithm modified for handling the size adaptability. This strategy allows the robot to access the narrow spaces with a smaller size while covering uncluttered areas with a larger size. Therefore, the proposed robot design can remarkably improve productivity in terms of area coverage and coverage time, which are crucial performance indicators for robots targeted for coverage applications. This fact has been verified through experimentally comparing the proposed reconfigurable design against robots with fixed morphology sizes. Exploration of ways to improve energy efficiency in addition to area coverage and coverage time is proposed for future work.

References

[1] P. N. Atkar, A. Greenfield, D. C. Conner, H. Choset, and A. A. Rizzi, "Uniform coverage of automotive surface patches," *The International Journal of Robotics Research*, vol. 24, no. 11, pp. 883–898, 2005.

[2] M. A. Yakoubi and M. T. Laskri, "The path planning of cleaner robot for coverage region using genetic algorithms," *Journal of innovation in digital ecosystems*, vol. 3, no. 1, pp. 37–43, 2016.

[3] E. U. Acar, H. Choset, Y. Zhang, and M. Schervish, "Path planning for robotic demining: Robust sensor-based coverage of unstructured environments and probabilistic methods," *The International journal of robotics research*, vol. 22, no. 7-8, pp. 441–466, 2003.

[4] Z. H. Khan, A. Siddique, and C. W. Lee, "Robotics utilization for healthcare digitization in global covid-19 management," *International journal of environmental research and public health*, vol. 17, no. 11, p. 3819, 2020.

[5] I. A. Hameed, "Intelligent coverage path planning for agricultural robots and autonomous machines on three-dimensional terrain," *Journal of Intelligent & Robotic Systems*, vol. 74, no. 3, pp. 965–983, 2014.

[6] K. Zheng, G. Chen, G. Cui, Y. Chen, F. Wu, and X. Chen, "Performance metrics for coverage of cleaning robots with mocap system," in *Int. Conf. Intelligent Robotics and Applications*. Springer, 2017, pp. 267–274.

[7] M. A. V. J. Muthugala, S. M. B. P. Samarakoon, and M. R. Elara, "Tradeoff between area coverage and energy usage of a self-reconfigurable floor cleaning robot based on user preference," *IEEE Access*, vol. 8, pp. 76 267–76 275, 2020.

[8] S. Rhim, J.-C. Ryu, K.-H. Park, and S.-G. Lee, "Performance evaluation criteria for autonomous cleaning robots," in *2007 Int. Symp. Computational Intelligence in Robotics and Automation*. IEEE, 2007, pp. 167–172.

[9] E. Galceran and M. Carreras, "A survey on coverage path planning for robotics," *Robotics and Autonomous systems*, vol. 61, no. 12, pp. 1258–1276, 2013.

[10] R. Bormann, F. Jordan, J. Hampp, and M. Hägele, "Indoor coverage path planning: Survey, implementation, analysis," in *2018 IEEE Int. Conf. Robotics and Automation (ICRA)*. IEEE, 2018, pp. 1718–1725.

[11] C. Luo, S. X. Yang, X. Li, and M. Q.-H. Meng, "Neural-dynamics-driven complete area coverage navigation through cooperation of multiple mobile robots," *IEEE Trans. Ind. Electron.*, vol. 64, no. 1, pp. 750–760, 2016.

[12] K. Guruprasad and T. Ranjitha, "Cpc algorithm: Exact area coverage by a mobile robot using approximate cellular decomposition," *Robotica*, vol. 39, no. 7, pp. 1141–1162, 2021.

[13] S. Bochkarev and S. L. Smith, "On minimizing turns in robot coverage path planning," in *2016 IEEE Int. Conf. Automation Science and Engineering (CASE)*. IEEE, 2016, pp. 1237–1242.

[14] I. Shnaps and E. Rimon, "Online coverage of planar environments by a battery powered autonomous mobile robot," *IEEE Trans. Autom. Sci. Eng*, vol. 13, no. 2, pp. 425–436, 2016.

[15] A. C. Kapoutsis, S. A. Chatzichristofis, and E. B. Kosmatopoulos, "Darp: divide areas algorithm for optimal multi-robot coverage path planning," *Journal of Intelligent & Robotic Systems*, vol. 86, no. 3-4, pp. 663–680, 2017.

[16] M. Yim, W.-M. Shen, B. Salemi, D. Rus, M. Moll, H. Lipson, E. Klavins, and G. S. Chirikjian, "Modular self-reconfigurable robot systems [grand challenges of robotics]," *IEEE Robotics & Automation Magazine*, vol. 14, no. 1, pp. 43–52, 2007.

[17] S. M. B. P. Samarakoon, M. A. V. J. Muthugala, R. E. Abdulkader, S. W. Si, T. T. Tun, and M. R. Elara, "Modelling and control of a reconfigurable robot for achieving reconfiguration and locomotion with different shapes," *Sensors*, vol. 21, no. 16, p. 5362, 2021.

[18] S. M. B. P. Samarakoon, M. A. V. J. Muthugala, and M. R. Elara, "Toward obstacle-specific morphology for a reconfigurable tiling robot," *Journal of Ambient Intelligence and Humanized Computing*, pp. 1–13, 2021.

[19] S. M. B. P. Samarakoon, M. A. V. J. Muthugala, M. R. Elara *et al.*, "Toward pleomorphic reconfigurable robots for optimum coverage," *Complexity*, vol. 2021, 2021.

[20] J. Seo, J. Paik, and M. Yim, "Modular reconfigurable robotics," *Annual Review of Control, Robotics, and Autonomous Systems*, vol. 2, pp. 63–88, 2019.

[21] J. Bae, S. Park, M. Yim, and T. Seo, "Polygon-based random tree search algorithm for a size-changing robot," *IEEE Robotics and Automation Letters*, 2021.

[22] W. K. Chung, L.-C. Fu, and T. Kröger, "Motion control," in *Springer handbook of robotics*. Springer, 2016, pp. 163–194.

[23] W. Li, C. Yang, Y. Jiang, X. Liu, and C.-Y. Su, "Motion planning for omnidirectional wheeled mobile robot by potential field method," *Journal of Advanced Transportation*, vol. 2017, 2017.

[24] A. Ntawumenyikizaba, H. H. Viet, and T. Chung, "An online complete coverage algorithm for cleaning robots based on boustrophedon motions and a* search," in *2012 8th Int. Conf. Information Science and Digital Content Technology (ICIDT2012)*, vol. 2. IEEE, 2012, pp. 401–405.